Journal of Applied Engineering and Technological Science
Vol 6(1) 2024: 444-464

A SUSTAINABLE HYBRID OFF-GRID SYSTEM DESIGN FOR ISOLATED ISLAND CONSIDERING TECHNO-ECONOMIC AND FREQUENCY STABILITY ANALYSIS

Candra Febri Nugraha[1*], Lukman Subekti[2], Ahmad Adhiim Muthahhari[3], Budi Eko Prasetyo[4], Rizki Firmansyah Setya Budi[5]
Department of Electrical Engineering and Informatics, Universitas Gadjah Mada, Indonesia[123]
Department of Electrical Engineering, Politeknik Negeri Malang, Indonesia[4]
Research Center for Nuclear Reactor Technology, National Research and Innovation Agency, Indonesia[5]
candra.febri.nugraha@ugm.ac.id

Received: 25 April 2024, Revised: 29 August 2024, Accepted: 06 September 2024
**Corresponding Author*

ABSTRACT
Electrifying remote islands presents complex challenges. Currently, most remote areas in Indonesia rely on diesel fuel for their electricity supplies, contributing to escalating generation costs and environmental degradation. Aligned with the global net-zero emission goal, this study proposes the design of a hybrid off-grid system for Kabare Village in the Raja Ampat Islands, integrating techno-economic and frequency stability analyses. HOMER Pro was employed to identify the most optimal system configuration, while DIgSILENT PowerFactory was utilized to assess the frequency stability performance of the system. This study unveils that the optimal system combines existing generators, solar panels, and batteries, with a net present cost of $1.37 million. The optimal system delivers an 11.8% reduction in levelized cost of energy to $0.269/kWh, alongside a 25.6% decrease in both fuel consumption and greenhouse gas emissions compared to the existing system. Moreover, the system meets frequency stability metrics, even under extreme operational conditions. This study demonstrates that implementing a hybrid off-grid system in Kabare Village is not only technically and economically feasible but also a practical option. These findings are anticipated to assist the government in promoting the utilization of renewable energy sources, particularly in remote areas such as the islands of eastern Indonesia.
Keywords : *Frequency Stability, Isolated Area, Off-Grid Hybrid, Power System Assessment, System Planning, Techno-Economic Analysis.*

1. Introduction

Indonesia, an archipelago of over 17,000 islands and a population of 275 million people (World Bank, 2022). While boasting an impressive national electrification rate of 97.63% in 2022 (PT PLN (Persero), 2023), this statistic masks a significant disparity. Eastern provinces like Papua and West Papua, characterized by dispersed communities across islands, lag far behind, with access rates as low as 62.85% (PT PLN (Persero), 2023). Addressing these disparities involves overcoming technical, social, economic, and social challenges (Matsumoto & Matsumura, 2022).

In remote areas, extending the main electricity grid is often impractical, making off-grid electrification a common alternative (Alqahtani & Patino-Echeverri, 2023; Setyowati, 2020). However, these isolated systems currently rely heavily on fossil fuel-based power generation, raising concerns about environmental impact. For instance, fossil fuels for 75% to 100% of electricity generation in the eastern provinces in 2022 (PT PLN (Persero), 2023). The Indonesian government's de-dieselization program seeks to replace diesel generators with renewable energy sources to promote sustainability (Syafrianto et al., 2021).

Off-grid hybrid systems combining renewable energy sources with energy storage present a viable solution for remote communities (Zebra et al., 2021). Previous research on off-grid hybrid systems focuses on identifying the most cost-effective configurations. HOMER Pro is a widely used tool for optimizing hybrid energy systems through techno-economic analysis. Some researchers have focused on developing grid-connected hybrid energy systems (Elhassan, 2023; Mehta & Basak, 2020), while others have explored the potential implementation of hybrid systems in specific locations, such as hospitals (Ahmed et al., 2023), educational institutions

(Alhawsawi et al., 2023). Hybrid systems can also be implemented in off-grid scenarios by utilizing local energy sources to provide sustainable energy supplies for remote areas, including remote mining sites (Ampah et al., 2023) and remote islands (Roy, 2023; Subekti et al., 2024).

Besides techno-economic assessment, some researchers have incorporated power system analyses to assess the technical feasibility of hybrid system projects by performing power flow analysis (Barco-Jiménez et al., 2022) and short-circuit analysis (Simic et al., 2021). Shezan et al. (2022) and Ishraque et al. (2022) performed more advanced analysis by evaluating dynamic power system stability, including voltage and power response.

No previous research on off-grid systems has combined techno-economic evaluations with comprehensive frequency stability analysis under various scenarios. This study aims to fill that gap by offering a holistic approach to evaluate both the techno-economic aspects and the frequency stability of an off-grid system, considering multiple scenarios. This study hypothesizes that the hybrid system will be more economically feasible compared to the conventional configuration and that the frequency stability analysis will demonstrate how the system responds to frequency instability events. Kabare Island in West Papua, Indonesia, is used as a case study to explore these issues in depth. This research offers unique contributions compared to prior studies, as outlined below:

1. Highlighting the techno-economic considerations for designing an off-grid system in the isolated context of Kabare Island.
2. Identifying the optimal system configuration to meet electricity demand and minimize dependence on fossil fuels in this specific region.
3. Conducting a thorough assessment of the frequency stability of the designed off-grid system using multiple operating scenarios.

This section explores deeper into the specifics of this research, followed by a literature review from previous studies in Section II. Section III details the study location, data collected, and the simulation setup. Section IV then presents the results of the study, followed by the concluding remarks in Section V.

2. Literature Review

2.1. Off-Grid Hybrid System Techno-Economic Analysis

The growing demand for sustainable and reliable energy sources has driven research towards decentralized power generation solutions like hybrid microgrids. The core principle of off-grid hybrid systems lies in integrating renewable and non-renewable energy sources, alongside energy storage (López-Castrillón et al., 2021). By utilizing local renewable resources, such as solar photovoltaic (PV), wind turbine (WT), micro-hydro, and biomass these systems can reduce dependence on expensive fossil fuels, making them economically viable options for remote communities (See et al., 2022).

Indonesia has abundant solar energy resources, making PV systems a critical component of off-grid hybrid energy solutions. Several studies have highlighted the significant role of PV in such systems. For instance, Riayatsyah et al., (2022) optimized a hybrid renewable energy system on Teupah Island, demonstrating that a 274 kW solar PV installation could contribute up to 29.2% of the energy mix, reducing the levelized cost of electricity (CoE) by 15.8%. In our previous research, we addressed the challenges of sustainable electricity supply in remote Indonesian islands, focusing on Yensawai Village in the Raja Ampat Islands (Subekti et al., 2024). The study identified an optimal configuration that included 70.1 kW of solar PV, resulting in a 29.6% renewable energy contribution and a 15.7% reduction in the levelized CoE.

While PV systems have shown considerable promise, other renewable energy sources, such as wind turbines, have also been explored. Kanata et al. (2021) found that wind turbines, although included in their optimal configuration with 4 kW capacity, contributed only 0.9% to the total generation, with PV dominating at 52%. However, an interesting finding by A. Xu et al. (2023) suggests that wind turbines can be more viable in specific locations, as evidenced by their 42% contribution to energy generation in Ponorogo Regency.

While techno-economic analysis is crucial in identifying the optimal configuration for hybrid systems, as demonstrated in prior research, it often provides an incomplete perspective. Utilizing HOMER Pro for this analysis is inadequate because its technical considerations are largely confined to simplified energy balance and resource availability, without thoroughly addressing essential factors such as power flow and system stability. To achieve an optimal and sustainable hybrid system design, a more comprehensive approach is required—one that integrates detailed technical assessments alongside economic evaluations.

2.2. Power System Assessment on System Planning

Beyond technological and economic factors, the design of power systems necessitates a comprehensive technical evaluation through detailed power system analyses. This assessment is a critical phase in power system design, aimed at determining the system's resilience to a range of potential contingency scenarios, thereby ensuring continuous operation under challenging conditions (Gholami et al., 2020). Power system analysis integrates both static and dynamic assessments, each offering valuable performance metrics (Kwon et al., 2020).

Power system static analysis involves evaluating an electrical power system under steady-state conditions, where parameters such as voltages, currents, and power flows are considered constant over time. This type of analysis focuses on the system's equilibrium state. A key method used in static analysis is load flow analysis, which determines voltage, current, and power flows and is essential for system planning, including the integration of renewable energy sources. For instance, Putranto et al. (2021) examined transmission system load flow in the context of long-term planning for high renewable energy penetration, concentrating on bus voltages and transmission line loading. Similarly, Hawas et al. (2022) assessed the impact of PV integration on distribution systems by analyzing bus voltage and component loading using DigSILENT PowerFactory. Barco-Jiménez et al. (2022) also explored PV power generation's effects on bus voltage profiles and losses in a microgrid, highlighting that PV generation can induce voltage fluctuations across the system.

In addition to static analysis, dynamic analysis plays a crucial role in power system planning by assessing the system's behavior during transient periods. Dynamic analysis encompasses voltage and frequency stability studies, which have garnered significant attention among researchers in recent years. For instance, Cárdenas Guerra et al. (2023) examined the impact of variable renewable energy (VRE) on power system dynamic stability, particularly focusing on voltage and frequency. Their findings suggest that integrating VRE into the power system may lead to voltage and frequency fluctuations. Similarly, Ishraque et al. (2022) investigated the voltage and power response of a microgrid with substantial VRE penetration and battery storage. Despite the high VRE penetration, their results indicate satisfactory dynamic stability, underscoring the stabilizing influence of battery storage as renewable energy sources increase (Aryani et al., 2022). Azhar et al. (2020) further explored the potential of battery energy storage systems (BESS) to mitigate the adverse effects of PV power intermittency by evaluating the frequency response. Their study demonstrates that the implementation of BESS can maintain the frequency nadir and rate-of-change of frequency (RoCoF) even under conditions of significant power loss.

However, previous studies have overlooked comprehensive frequency stability analysis, particularly in the context of off-grid system planning. The present study aims to evaluate both the techno-economic and technical aspects, with a specific focus on frequency stability analysis in off-grid systems. Frequency stability analysis is increasingly critical when examining off-grid systems due to the absence of grid connections, which can result in a lack of voltage and frequency support, as well as insufficient inertia (G. Xu et al., 2021). Consequently, ensuring stability in off-grid systems is essential during the design phase.

3. Research Methods

3.1. Study Case: Kabare Village

This study focuses on the village of Kabare, located on Waigeo Island within the Raja Ampat Islands, an Indonesian archipelagic region encompassing over 600 islands and spanning a total area of 67,379.60 km² (Badan Pusatat Statistik Kabupaten Raja Ampat, 2020). The scattered small villages that characterize the landscape are exemplified by Kabare, which currently relies on two diesel generators (100 kW and 80 kW) to meet its electricity needs. Fig. 2 depicts the island and village location.

Fig. 1. The location of Kabare Village.

Kabare's electricity consumption pattern obtained from a primary source, illustrated in Fig. 3, exhibits a distinct profile. Demand is highest in the early morning, followed by a decrease during the day and a gradual rise towards the evening with a peak load of 69 kW. This pattern aligns with the dominance of household loads in the area, resulting in significantly higher energy consumption during times of peak household activity, such as early mornings and evenings.

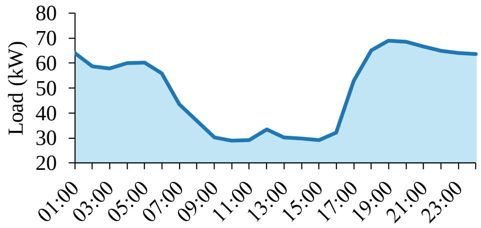

Fig. 2. Average electrical load demand.

The selection of suitable renewable energy sources for a specific region relies heavily on its meteorological characteristics. A comprehensive assessment considering data like global horizontal irradiation (GHI), temperature, and wind speed is crucial for accurately evaluating the potential of different renewable resources. This study utilizes NASA data for GHI and temperature, integrated into HOMER Pro software (Fig. 3 and Fig. 4). The average daily solar irradiation is 4.61 kWh/m², and the average annual temperature is 27.22 °C. Wind speed data, acquired through field measurements, averages 3.21 m/s, as shown in Fig. 5.

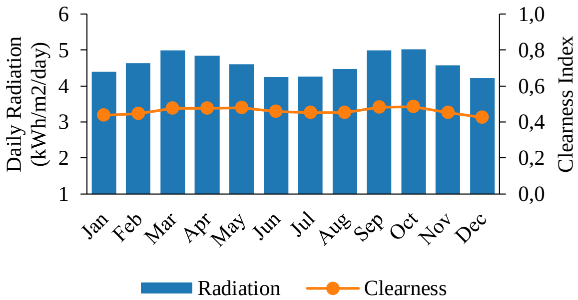

Fig. 3. Daily radiation and clearness index profile (National Aeronautics and Space Administration (NASA) Langley Research Center (LRac), 2022).

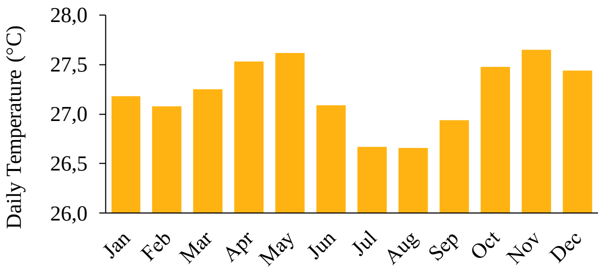

Fig. 4. Daily temperature profile (National Aeronautics and Space Administration (NASA) Langley Research Center (LRac), 2022).

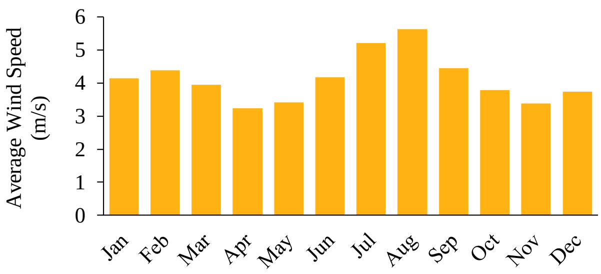

Fig. 5. Average wind speed profile.

3.2. Research Workflow

The research workflow, presented in Fig. 6, comprises two key stages: determining the optimal system configuration and evaluating its frequency stability. Techno-economic analysis of various configurations employed HOMER Pro, while frequency stability assessment utilized DIgSILENT PowerFactory.

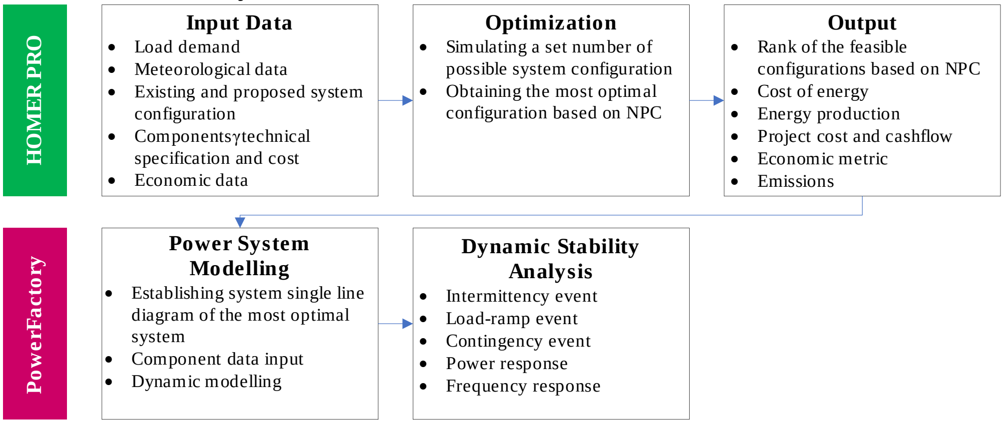

Fig. 6. Research workflow.

The research began with data collection for hybrid off-grid system optimization, including electrical load demand, meteorological data (solar radiation, temperature, wind speed), existing system details, component specifications and costs, and economic data. Subsequently, the proposed system configuration was modeled and evaluated through simulations encompassing numerous possible configurations to identify the most optimal configuration based on net present cost (NPC). This yielded feasible configurations ranked by NPC and levelized cost of energy (CoE). The configuration with the lowest NPC was then chosen for further analysis using power system analysis tools.

DIgSILENT PowerFactory supported the modeling and simulation of this chosen configuration. This involved creating a single-line diagram, inputting component technical data and dynamic parameters, and then conducting power system simulations by triggering stability events to observe the system's frequency response.

3.3. Techno-Economic Analysis of Off-Grid System Configuration

Fig. 7 depicts the proposed system configuration, which incorporates both alternating current (AC) and direct current (DC) voltages. Loads are connected to the AC bus, designed with a higher peak capacity than the existing data to account for potential load fluctuations. Existing generators, wind turbine candidates, and solar PV candidates are all connected to the AC bus. To ensure proper integration, the solar PV system is connected to the AC bus through a dedicated inverter, while the battery system operates solely on the dedicated DC bus. These two buses are then linked by converters to facilitate the flow of energy between them.

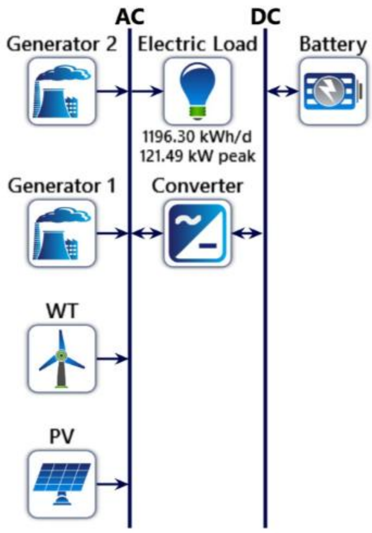

Fig. 7. Proposed system configuration.

3.3.1. Diesel Generator

The generator's fuel consumption, which defines the amount of fuel needed to generate electricity, is represented by a fuel curve. This curve can be expressed mathematically as a function of the generator's electrical output, as shown in Equation (1) (HOMER Energy, 2017).

$$F = F_0 Y_{gen} + F_1 P_{gen} \tag{1}$$

Table 1 summarizes the technical and economic data of the existing generators. The listed "lifetime" indicates the operating timeframe before a major overhaul becomes necessary, while the "replacement cost" refers to the associated overhaul expense. The diesel generator fuel cost is assumed to be \$0.84/l, estimated based on field report by PT PLN (Persero) (2020).

Table 1 - Diesel generator techno-economic data (HOMER Energy, 2017).

Specifications	Unit	Value
Generator 1		
Capacity	kW	100
Min. load ratio	%	6
Min. runtime	minutes	60
Fuel curve intercept coefficient	l/hr/kW rated	0.028
Fuel curve slope	l/hr/kW output	0.253
Replacement cost	$	5.500
O&M cost	$/op. hour	2.0
Lifetime	op. hour	20,000
Generator 2		
Capacity	kW	80
Min. load ratio	%	6
Min. runtime	minutes	60
Fuel curve intercept coefficient	l/hr/kW rated	0.033
Fuel curve slope	l/hr/kW output	0.273
Replacement cost	$	3,750
O&M cost	$/op. hour	1.6
Lifetime	op. hour	20,000
Fuel		
Fuel Cost	$/l	0.84

3.3.2. Solar Photovoltaic

The power output of the PV system is determined through an analysis that considers various factors affecting production. This analysis is often represented mathematically, as shown in Equation (2) (HOMER Energy, 2017). One key factor is the derating factor, which represents the ratio between the actual power output of a panel and its rated capacity. This value can be impacted by factors like shading, soiling, and inherent system losses. Additionally, the solar irradiance, or the amount of solar radiation directly striking the panel's surface, directly influences its power output. Finally, the temperature coefficient plays a crucial role. As described by Equation (2), the power output of a panel generally decreases as its temperature rises.

Table *2* presents the photovoltaic data used in the simulation, including details relevant to these factors.

$$P_{PV} = Y_{PV} f_{PV} \left(\frac{\bar{G}_T}{\bar{G}_{T,STC}} \right) \left[1 + \alpha_P (T_c - T_{c,STC}) \right] \tag{2}$$

Table 2 - Photovoltaic techno-economic data (Trina Solar Limited, 2020).

Specification	Unit	Value
Solar Panel		
Peak power	Wp	380
Maximum power voltage	V	34.7
Maximum power current	A	10.96
Open circuit voltage	V	41.9
Short circuit current	A	11.52
Module efficiency	%	20.7
Temperature coefficient	%/°C	-0.34
Normal operating cell temperature	°C	43
Derating factor	%	88
Capital cost	$	354
Replacement cost	$/year	354
O&M cost	$/year	5.5
Lifetime	years	25
Solar Inverter		
Power rating	kW	125
Capital cost	$	13,289
Replacement cost	$	13,289
Lifetime	years	15

3.3.3. Wind Turbine

Wind turbine power output is determined by two factors: wind speed and the turbine's power curve. However, wind speed measurements often differ from the actual hub height where the turbine operates. To address this discrepancy, HOMER Pro employs a logarithmic equation, as shown in Equation (3), to predict the wind speed at the hub height (HOMER Energy, 2017).

$$U_{hub} = U_{anem} \frac{\ln(z_{hub}/z_0)}{\ln(z_{anem}/z_0)} \tag{3}$$

Once the hub height wind speed is established, HOMER Pro utilizes the power curve, as shown in Fig. 8, to calculate the expected power output at standard temperature and pressure (STP) conditions. This power curve depicts the relationship between wind speed and the corresponding power generation. To account for real-world variations in air density, HOMER Pro further adjusts the predicted power using an air density ratio, calculated using Equation (4) (HOMER Energy, 2017).

Table *3* summarizes the wind turbine data employed in the simulation.

$$P_{WTG} = \left(\frac{\rho}{\rho_0} \right) P_{WTG,STP} \tag{4}$$

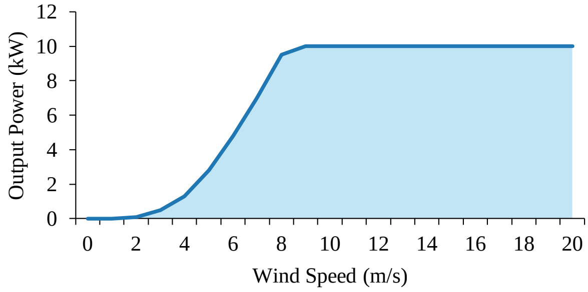

Fig. 8. Wind turbine power curve (Ryse Energy, 2020).

Table 3 - Wind turbine techno-economic data (Renugen, 2024; Ryse Energy, 2020).

Specification	Unit	Value
Power rating	kW	10
Hub height	m	30
Capital cost	$	63,952
Replacement cost	$	25,581
O&M cost	$/year	56
Lifetime	years	20

3.3.4. Battery Storage

The proposed configuration employs Lithium-ion batteries, each with a capacity of 1 kWh and a voltage of 6 V. Determining the required number of batteries in series involves considering the converter's acceptable input voltage range. For this system, a 480 V DC bus voltage was selected, enabling a series connection of 80 batteries. The detailed battery data used in the simulation is provided in Table 4.

Table 4 - Battery techno-economic data (HOMER Energy, 2017).

Specification	Unit	Value
Capacity	kWh	1
Energy throughput	kWh	3,000
Initial SoC	%	100
Min. SoC	%	20
Capital cost	$	550
Replacement cost	$	550
O&M cost	$/year	10
Lifetime	years	15

3.3.5. Battery Converter

Converter selection prioritized control capabilities due to the system's isolated nature. In an isolated system, maintaining voltage and frequency is crucial to avoid power disruptions. While generators can fulfill this role, their continuous operation incurs high fuel costs, prompting the need for alternative solutions.

Research in this field suggests that inverters with "grid-forming" capabilities can effectively regulate both voltage and frequency in isolated systems, enabling them to function independently without relying on external grids or backup generators (Lasseter et al., 2020; Rathnayake et al., 2021). This capability allows for "black starts," where the system can be restarted without external assistance.

Based on these considerations, a 30-kW bi-directional battery converter with built-in grid-forming capabilities was chosen for this study. This converter is compatible with various batteries, including lead-acid, lithium, and sodium-ion, and accepts a wide voltage range of 150 to 750 V. The detailed specifications of this converter are presented in Table 5.

Table 5 - Battery converter techno-economic data (HOMER Energy, 2017).

Specification	Unit	Value
Capacity	kW	30
Efficiency	%	95
Capital cost	$	10,000
Replacement cost	$	10,000
Lifetime	years	15

3.4. Economic Analysis

In the HOMER Pro economic analysis, several assumptions were made, encompassing the inflation rate, nominal discount rate, and project lifetime, as detailed in Table 6. The definitions of the economic terms are provided below.

Table 6 - The assumption of macroeconomic data (Bank Indonesia, 2023).

Parameter	Unit	Value
Inflation rate	%	3
Nominal discount rate	%	9
Project lifetime	years	25
Replacement cost	$	10,000
Lifetime	years	15

3.4.1. Discount Rate

The real discount rate, which is the discount rate used to convert one-time expenses to annualized costs using Equation (5), is calculated by HOMER Pro. Where: i representing the real discount rate, i' representing the nominal discount rate, and f representing the expected inflation rate (HOMER Energy, 2017).

$$i = \frac{i' - f}{1 + f} \tag{5}$$

3.3.2. Net Present Cost

The net present cost (NPC) serves as a crucial metric for evaluating the economic feasibility of a project. It represents the difference between the present value of all project expenses and the present value of all project revenues generated throughout the project's lifespan.

Project expenses encompass costs related to construction, operation, and maintenance, while potential salvage value from equipment at the project's end is considered revenue. Equation (6) (HOMER Energy, 2017) can be used to calculate the NPC.

$$NPC = -C_{cap} + \sum_{n=0}^{R_{proj}} \frac{C_n}{(1 + i)^{R_{proj}}} \tag{6}$$

3.3.3. Levelized Cost of Energy

In addition to the NPC, another critical economic metric is the levelized cost of energy (CoE), typically expressed in units of $/kWh. Unlike the NPC which considers the total project cost, the CoE reflects the average cost per unit of energy delivered over the project's lifetime. As shown in Equation (7), HOMER Pro determines the CoE by dividing the yearly cost of generating electricity by the total energy supplied to the system. (HOMER Energy, 2017).

$$COE = \frac{C_{ann,tot}}{E_{served}} \tag{7}$$

3.4.4. Internal Rate of Return

The internal rate of return (IRR) represents the discount rate that makes the NPC of the base case and the optimized scenarios equal. HOMER Pro calculates the IRR by identifying the discount rate that makes the NPV of the difference between the two cash flows equal to zero (HOMER Energy, 2017).

3.4.5. Payback Period

The payback period indicates the timeframe required for the total project income to equal the initial investment. This period is often used as a simple indicator of a project's investment recovery rate. This allows for a quick comparison of the investment recovery potential associated with implementing the optimized system.

3.5. Frequency Stability Analysis

Frequency stability refers to the system's ability to sustain the frequency at its nominal value despite disturbances (Denholm et al., 2020). The swing equation, presented in Equation (8), expresses a power system frequency dynamics following a power imbalance between generation and load (Chavez et al., 2014; Kundur, 2007). Fig. 9 depicts a typical frequency response of a system experiencing a power imbalance. The system's inertia and governor droop primarily determine the power grid's frequency response to imbalances between generation and load. (Atkinson & Albayati, 2021).

$$\frac{df(t)}{dt} = \frac{1}{M_H}(P_m(t) - P_e(t)) \tag{8}$$

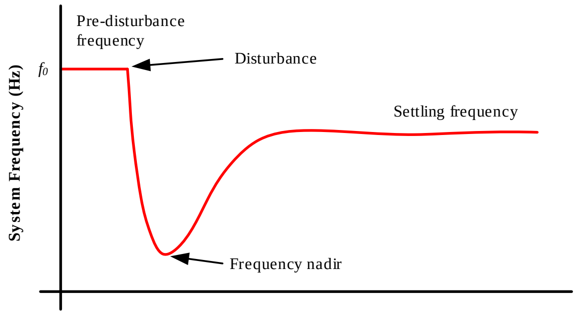

Fig. 9. Frequency response following a disturbance.

Parameters derived from the frequency response, such as the frequency nadir (the lowest observed frequency), are vital indicators of the system's frequency stability (Chamorro et al., 2020). According to the standards outlined in (Russian Federation, 2014), isolated systems must uphold the frequency deviation within ±1 Hz for 95% of the one-week operation interval and within ±5 Hz for the entire duration.

The system's frequency stability was assessed through simulations mimicking various power imbalance events, including intermittency in renewable generation, sudden increases in demand, and generator outages. These simulations were run under diverse operating conditions, and the specific scenarios considered are described below.

3.5.1. Operating Scenario 1

Intermittency from renewable sources like solar and wind can impact frequency stability. This scenario simulates the system's response to sudden drops in power output during high renewable penetration, mimicking extreme events observed locally. Fig. 10 and Fig. 11 depict the intermittency patterns, emphasizing the simulated power reductions. This test was designed to assess the system's ability to handle rapid renewable fluctuations.

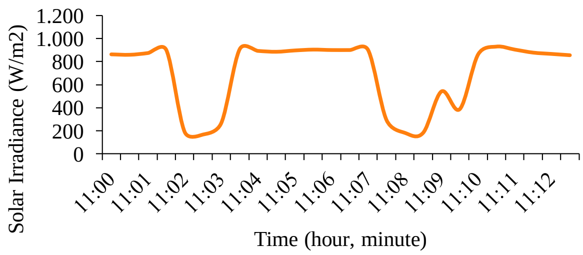

Fig. 10. Recorded solar irradiance fluctuation.

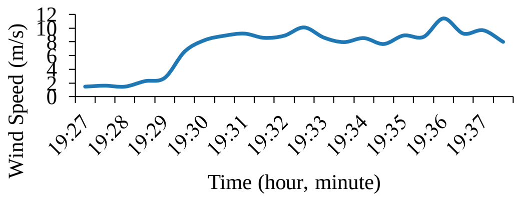

Fig. 11. Recorded wind speed fluctuation.

3.5.2. Operating Scenario 2

To ensure robust performance under demanding circumstances, two critical test cases were simulated and analyzed. The first investigated the system's response to surpassing its annual peak demand. This simulated a sudden surge in electricity consumption exceeding the level observed on the day with the highest yearly load. This test assessed the system's ability to handle unexpected spikes in power requirements that could potentially exceed its anticipated capacity.

Additionally, a generator outage under peak load test was conducted. This mimicked a sudden loss of generation capacity, such as from equipment malfunction or other unforeseen disturbances, during the system's annual peak load condition. This evaluated the system's resilience and ability to maintain frequency stability despite losing a critical generation source during a period of high demand.

4. Results and Discussions

4.1. Optimal Configuration

Utilizing HOMER Pro software, the study optimized the system configuration by analyzing a set of pre-defined component options that met technical and economic requirements. Each configuration was evaluated based on the NPC, with the top five ranked options presented in Table 7. The optimal configuration emerged as a combination of existing generator sets, a 126 kW PV system, a 60 kW inverter, and an 80 kWh battery bank. Notably, the wind turbine option was not selected due to the inadequate wind resource potential in the study area. This finding is consistent with our previous research (Subekti et al., 2024) conducted in a similar location, suggesting that wind energy remains unfeasible for implementation due to insufficient wind potential. Despite this, the optimized configuration achieved a respectable 22.7% share of renewable energy generation within the system, as indicated by the renewable energy generation fraction.

Table 7 also incorporates the base case scenario for comparison, which represents the existing system solely comprised of two diesel generators. This comparison provides context for the potential improvements achievable through optimization.

Table 7 - Top five system configurations.

Rank	Generator 1 (kW)	Generator 2 (kW)	PV (kW)	Wind Turbine (kW)	Battery (kWh)	Converter (kW)	NPC ($M)	CoE ($/kWh)	Ren. Frac. (%)
1	100	80	126.0	0	80	60	1.37	0.269	22.7
2	100	80	121.0	10	80	60	1.40	0.276	24.6
3	100	80	77.6	0	0	0	1.45	0.286	16.6
4	100	80	72.9	10	0	0	1.49	0.294	18.6
5	100	80	0.0	0	0	0	1.55	0.305	0

4.2. Electrical Energy Generation

A generation portfolio utilizing various sources, including diesel and PV, successfully met the system's year-round load demand. Fig. 12 displays the power output of generator 1 and generator 2 throughout the year. The horizontal axis represents the number of days, while the vertical axis represents the number of hours in a day. Color intensity reflects the generated power according to the scale on the right. Notably, Generator 1 operated more frequently, primarily during peak hours between 6 PM and 6 AM the following day. This resulted in 4,909 operational hours and an annual energy output of 310.1 MWh.

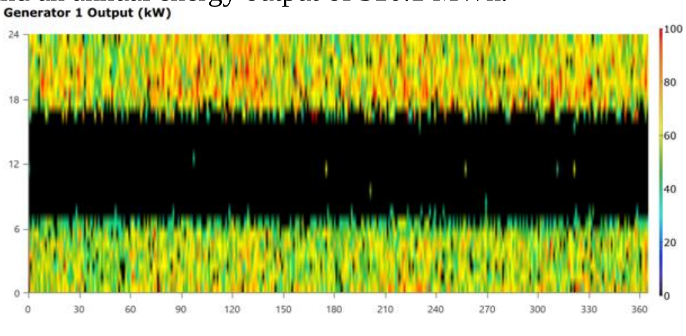

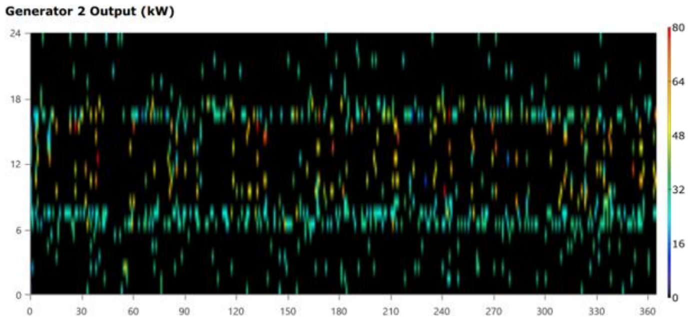

Fig. 12. Diesel generator electrical energy generation

In contrast, Generator 2 only operated for 734 hours, generating a total of 27.4 MWh annually. This information demonstrates the differentiated operation patterns and energy contributions of the two generators within the system. Typically, operating a single generator suffices to fulfill the demand, with the second unit providing redundancy and peak load support. While efficiency might be slightly higher with a single generator, the two-generator configuration may ensure system robustness in the event of an emergency.

Fig. 13 showcases the electrical energy generation profile of the photovoltaic (PV) system. While the installed capacity of the system is 126 kW, its observed peak output reaches 114 kW. Consistent with solar energy characteristics, power generation commences at sunrise (6 AM), peaks at noon, and tapers off by sunset (6 PM). This daily pattern translates to an annual energy production of 167.6 MWh, corresponding to a capacity factor (CF) of 15.1%. This CF falls within the expected range (15%-19%) for Indonesian provinces, as reported by the Ministry of Energy and Mineral Resources; Danish Energy Agency (2021). The observed CF suggests that the system is performing within the anticipated parameters for the region.

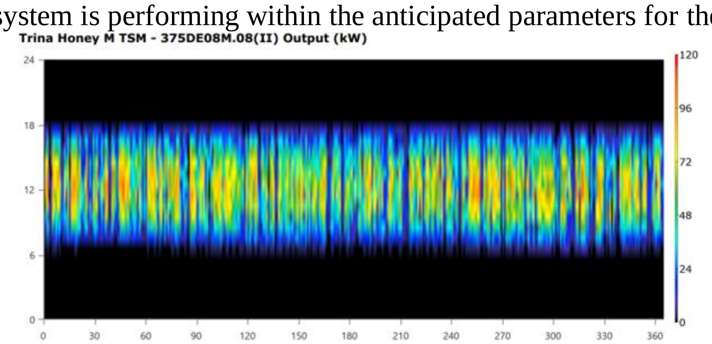

Fig. 13. PV electrical energy generation

Fig. 14 illustrates the breakdown of annual energy generation by source. While conventional sources, Generator 1 and Generator 2, collectively supplied 66.8% (61.4% and 5.4%, respectively), the integration of renewable energy played a crucial role, with the PV system contributing 33.2% of the total annual generation. This balance between conventional and renewable energy sources highlights the potential of hybrid systems to achieve both reliable and sustainable power generation.

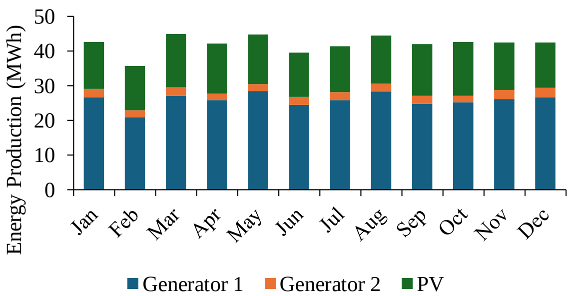

Fig. 14. Monthly electricity production

Fig. 15, utilizing a color scheme to represent the battery's state of charge (SoC) with details provided on the right, reveals a consistently high average SoC of 96.9% throughout the year. However, instances of lower SoC, primarily between 6 AM and 6 PM, were observed in response to the intermittent nature of PV power generation. During these periods, the 80-kWh battery discharged energy to compensate for the power deficit, ensuring the system's power balance. The battery's capacity to sustain the load for 1.28 hours in the event of an outage highlights its role in enhancing system resilience, also known as its autonomy duration. Notably, the battery achieved an annual energy throughput of 13,926 kWh while experiencing total losses of 1,468 kWh.

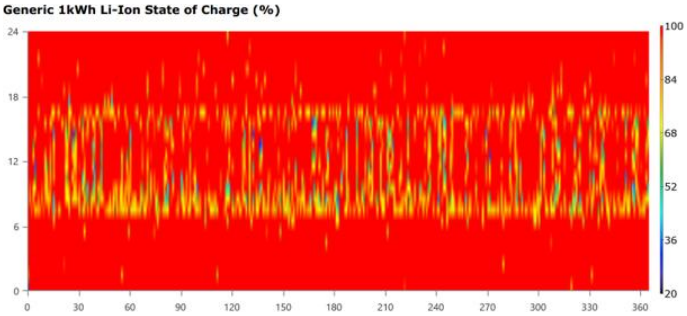

Fig. 15. Battery state of charge

4.3. Economic Evaluation

The economic analysis, detailed in Table 8, reveals significant financial benefits associated with the optimized system configuration compared to the base case scenario. While requiring an initial investment (CAPEX) of $195,027, the optimized configuration offers substantial cost savings in the long run. It achieves a lower NPC of $1.37 million compared to the base case's $1.55 million, translating to an 11.8% reduction in CoE from $0.305/kWh to $0.269/kWh. Additionally, lower annual operating and maintenance costs (OPEX) of $100,798 are observed compared to the base case's $133,153. These cost savings contribute significantly to the economic attractiveness of the optimized configuration, further emphasized by the comparative economic parameters summarized in

Table *9*.

Table 8 - NPV, CAPEX, and OPEX of the optimal and base case configuration.

Quantity	Base Case	Optimal
NPC ($M)	1.55	1.37
CoE ($/kWh)	0.305	0.269
CAPEX ($)	0	195,027
OPEX ($/year)	136,659	101,619

Table 9 - Comparative economy analysis between the base case and optimal configuration.

Parameter	Value
IRR (%)	15.7
Discounted payback (years)	7.31
Operation cost savings ($/year)	35,040

The optimized configuration boasts a short payback period of 7.31 years, indicating a swift recovery of the initial investment. Additionally, its strong financial return is evident from the IRR of 15.7%. Notably, the configuration reduces operating costs by a substantial 25.6%, translating to annual savings of $35,040 compared to the base case. These combined economic metrics strongly support the feasibility and financial attractiveness of the optimized system configuration.

Fig. 16 provides a breakdown of cost components associated with the optimal configuration, with fuel costs for Generator 1 accounting for the largest portion, followed by its operation and maintenance (O&M) costs. The initial investment cost of the PV system emerges as the third most significant cost component. This breakdown highlights the significant contribution of conventional fuel sources to the overall system cost, despite the inclusion of renewable energy.

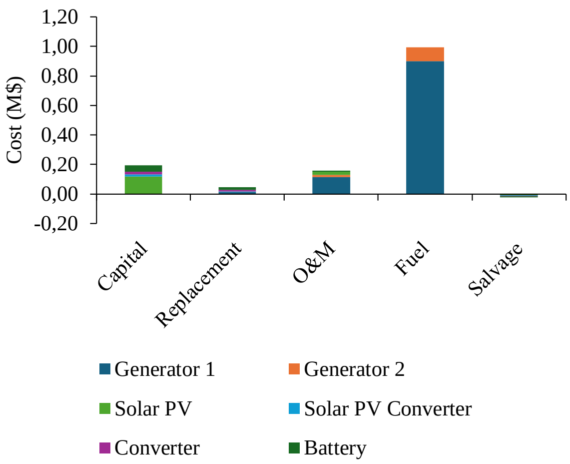

Fig. 16. Project cost components.

4.4. Environment Impact Evaluation

The optimal system configuration resulted in significant environmental benefits compared to the base case. Table 10 highlights this by showcasing the reductions in both fuel consumption and greenhouse gas (GHG) emissions. As the diesel generator served as the sole source of emissions, the observed decrease in fuel consumption directly translates to a proportional reduction in GHG production. This finding underlines the potential of the optimized configuration to deliver electricity more sustainably, achieving a 25% reduction in both fuel consumption and total emissions compared to the base case.

Table 10 - Fuel consumption and emissions produced in the base case and optimal configuration.

Quantity	Base Case	Optimal
Fuel consumption		
Diesel (l/year)	136,656	101,619
Emission (kg/year)		
Carbon dioxide	357,505	265,815
Carbon monoxide	2,386	1,795
Unburned hydrocarbons	98.4	73.2
Particulate matter	10.6	7.49
Sulfur dioxide	876	651
Nitrogen oxides	628	276
Total	361,504	268,618

4.5. Comparison with Previous Works

This section offers a comparative analysis between the findings of the current study and those of previous research on off-grid hybrid system optimization, particularly in isolated regions of Indonesia. Table 11 provides a detailed comparison of the results from earlier studies and the current research, focusing on critical aspects such as optimal configurations and economic metrics.

Table 11 – Comparison of presented work with previous research.

Authors	Study Case	Peak Load (kW)	Diesel Generator (kW)	PV (kW)	Wind Turbine (kW)	Battery (kWh)	CoE ($/kWh)
Kanata et al. (2021)	Sebesi Island	50.6	100.0	69.5	0	49.0	0.286
Riayatsyah et al., (2022)	Teupah Island	162.4	160.0	274.0	0	76.0	0.246
A. Xu et al., (2023)	Ponorogo	211.4	80.00	187.0	70	457.0	0.21
Subekti et al. (2024)	Yensawai	77.9	160.0	70.1	0	80.0	0.236
Presented work	Kabare	121.5	180	126	0	80	0.269

The findings consistently indicate that the most technically and economically viable configuration for off-grid hybrid systems typically includes a diesel generator, PV, and battery storage. In contrast, the inclusion of wind turbines is often excluded due to the potential for increased energy costs. This exclusion is primarily due to the insufficient wind resources observed in the studied locations. However, the study by (A. Xu et al., 2023) demonstrates that wind turbines can be viable in specific locations, as evidenced by the inclusion of a 70 kW wind turbine in their optimal configuration. Their findings attribute this viability to relatively higher wind speeds in the studied area, recorded at 4.28 m/s.

The optimal configurations identified in both previous studies and the current research result in energy costs ranging from \$0.21 to \$0.286/kWh. This variation can be attributed to several factors, including differing assumptions regarding technology prices, economic parameters, diesel costs, and meteorological data specific to each case study. Nevertheless, these hybrid systems remain more cost-effective compared to the diesel generation costs in Indonesia’s isolated systems, averaging at \$0.3/kWh, as reported by (PT PLN (Persero), 2020). This comparison underscores the economic viability of hybrid systems over conventional diesel generation.

It is important to note that Table 11 compares results across various case studies. Its primary purpose is not to highlight the effectiveness of the method presented in this study but to provide a broad comparison across different scenarios. Unlike prior studies, our research illustrates the technical and economic feasibility of implementing a hybrid off-grid system specifically tailored to the unique conditions of Kabare Village. This distinction emphasizes the novelty of our findings within a particular geographical context.

4.6. Frequency Stability Analysis

Based on the optimal design of the off-grid system was modeled in DIgSILENT PowerFactory. The single-line diagram of the system is depicted in Fig. 17. The PV, generator, and battery converter were connected to the AC bus. Additionally, the converter and the battery were integrated into a single component, which was also linked to the AC bus.

4.6.1. Operating Scenario 1

To evaluate the system's performance under extreme power intermittency conditions, a high PV generation day, occurring on February 16th at 11 AM, was chosen. This day also coincided with high power demand (53.6 kW). While the high PV generation (97.9 kW) exceeded the demand, it could not be fully utilized due to a full battery condition.

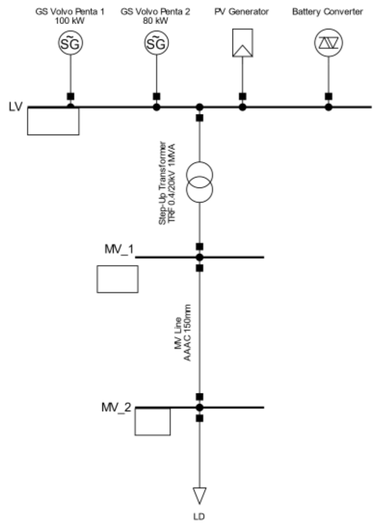

Fig. 17. System modeling in PowerFactory.

To assess the system's ability to handle extreme weather events, an intermittency event was simulated by reducing solar irradiation by 70% within 30 seconds. Fig. 18 illustrates the system's power and frequency response. As shown in the figure, the initial solar irradiation of 672.8 W/m^2 dropped to 201.8 W/m^2, leading to a decrease in PV power output from 56.0 kW to 13.5 kW. The battery system responded by increasing its output from 0 kW to 41.9 kW to compensate for the lost power. While this event resulted in a significant drop in frequency, reaching a nadir of 49.67 Hz, it remained above the minimum standard. This underscores the critical role of fast-response sources, such as battery systems, in maintaining system frequency during significant power losses, which is consistent with the findings of Azhar et al., (2020).

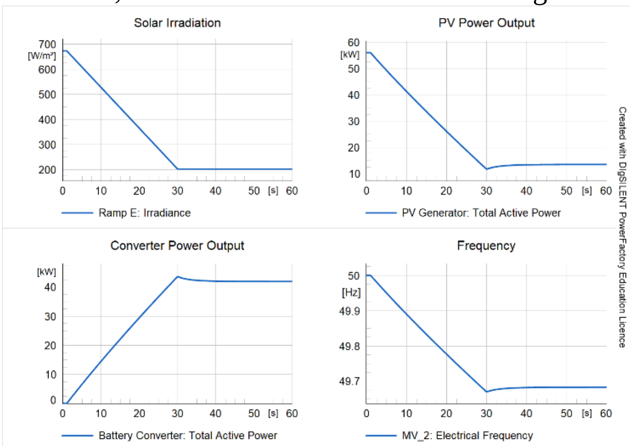

Fig. 18. System response after solar irradiation significantly dropped.

4.6.2. Operating Scenario 2

To understand how the system handles peak load situations, we analyzed a scenario representing the annual peak load, occurring on November 10th at 6 PM. Initially, the system had a load of 121.5 kW, with Generator 1 at full power and Generator 2 partially loaded. Solar panels were not generating, and the batteries were not supplying any power.

When the load suddenly increased by 10% over 10 seconds (see Fig. 19), both generators responded by increasing their output. However, because diesel generators take time to ramp up, the battery converter reacted faster by increasing its output from 0 kW to 2.8 kW to compensate temporarily. Once the generators' output reached the new set point, the converter stopped supplying power. The system's frequency dipped slightly to 49.98 Hz but quickly recovered to nominal frequency.

These findings also emphasize the crucial role of generators' frequency response via governors in maintaining system frequency. Bryant et al., (2021) note that high levels of governor inactivity can significantly compromise power system stability, particularly in systems with a high penetration of inverter-based renewable energy sources.

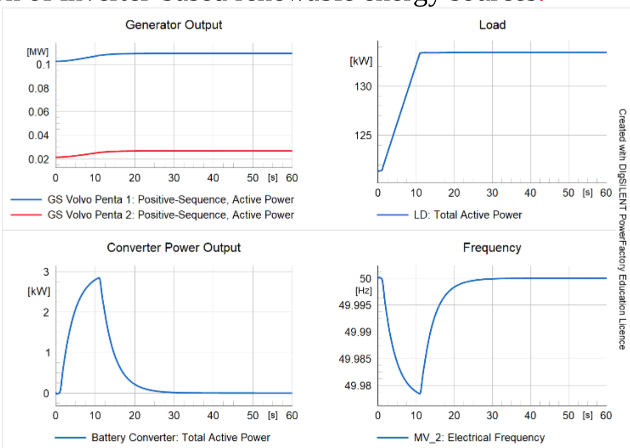

Fig. 19. System response after the load ramp.

To understand the system's capabilities further, an extreme event was simulated: a fault on the highest-loaded generator (Generator 1) on November 10th at 6 PM. This event not only imposes an additional burden on Generator 2 and battery storage due to the power loss but also further jeopardizes system stability due to inertia loss.

As shown in Fig. 20, when generator 1 tripped, both the remaining generator (Generator 2) and the battery converter responded rapidly to maintain power. Due to its slower response to faults, the generator initially couldn't fully compensate for the lost power. Consequently, the converter, initially inactive, surged to 75.7 kW to bridge the gap. As Generator 2 gradually ramped up its output, increasing from 21.5 kW to 87.6 kW, the converter's need to compensate decreased. However, since Generator 2 couldn't fully meet the entire demand alone, the converter continued supplying 33.7 kW to maintain system stability. Despite the sudden loss of a major power source, the system frequency only dipped to 49.32 Hz and then stabilized at 49.74 Hz.

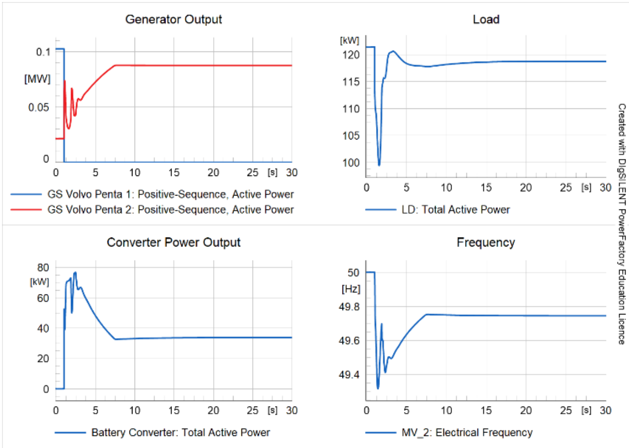

Fig. 20. System response after Generator 1 tripped.

5. Conclusion

Isolated power systems in Indonesia currently depend heavily on diesel fuel, resulting in high generation costs and significant greenhouse gas emissions. Off-grid hybrid systems, which integrate renewable and non-renewable energy sources, offer a promising alternative. While techno-economic analysis provides a preliminary assessment of feasibility, it alone is insufficient for ensuring system reliability. A comprehensive technical analysis, particularly focusing on stability, is essential in the design phase of off-grid hybrid systems, as these systems are more vulnerable to stability issues due to the lack of voltage and frequency support from a central grid.

This research presents a design for an off-grid hybrid system tailored for Kabare Village, Indonesia, incorporating a techno-economic perspective along with a thorough power system stability analysis, with an emphasis on frequency stability. The proposed optimal configuration consists of a 180 kW diesel generator, 126 kW PV, and an 80 kWh battery. This setup achieves an NPC of $1.37 million and a CoE of $0.269/kWh, which are both lower than those of a conventional configuration, which has an NPC of $1.55 million and a CoE of $0.305/kWh.

In addition to its economic advantages, the proposed system demonstrates robust frequency stability, maintaining frequency above 49 Hz even under challenging conditions, such as variable renewable energy output, significant load ramps, and generator trips. The simulation results show the critical role of the battery in frequency regulation, thanks to its fast-response characteristics.

Consequently, an independent hybrid system combining PV and batteries with backup diesel generation proves to be a technically sound, economically feasible, and practically viable solution for providing electricity to Kabare Village. This conclusion holds valuable implications for policymakers aiming to promote renewable energy adoption in remote regions of Indonesia. Future research should explore other aspects of system stability, such as dynamic voltage stability, which is also a critical metric for ensuring the overall stability of off-grid systems.

Nomenclature

F_0	fuel curve intercept coefficient (l/hr/kW rated)
F_1	fuel curve slope (l/hr/kW output)
Y_{gen}	generator's rated capacity (kW)
P_{gen}	generator's power output (kW)
Y_{PV}	rated capacity of the photovoltaic array under standard test conditions (kW)

f_{PV}	derating factor (%)
$\bar{G}_T$	solar irradiance hitting the PV array (kW/m^2)
$\bar{G}_{T,STC}$	solar irradiance under standard test conditions (1 kW/m^2)
α_P	temperature coefficient (%/°C)
T_c	temperature of the photovoltaic cell (°C)
$T_{c,STC}$	temperature of the photovoltaic cell under standard test conditions (25 °C)
P_{WTG}	wind turbine output power (kW)
$P_{WTG,STP}$	wind turbine output power at STP (kW)
ρ	real air density (kg/m^3)
ρ_0	real air density at STP (1.225 kg/m^3)
i	real discount rate (%)
i'	nominal discount rate (%)
f	expected inflation rate (%)
C_{cap}	capital cost of the selected system
C_n	nominal annual cash flow
R_{proj}	project lifetime (year)
$C_{ann,tot}$	system's total annualized cost ($/year)
E_{served}	electrical load served (kWh/year)
R_{proj}	project lifetime (year)
$f(t)$	system frequency at time t (Hz)
M_H	system inertia after generation loss (MWs/Hz)
$P_m(t)$	system mechanical power at time t (MW)
$P_e(t)$	system electrical load at time t (MW)

References

Ahmed, M. R., Hasan, M. R., Al Hasan, S., Aziz, M., & Hoque, M. E. (2023). Feasibility Study of the Grid-Connected Hybrid Energy System for Supplying Electricity to Support the Health and Education Sector in the Metropolitan Area. *Energies*, *16*(4). https://doi.org/10.3390/en16041571

Alhawsawi, E. Y., Habbi, H. M. D., Hawsawi, M., & Zohdy, M. A. (2023). Optimal Design and Operation of Hybrid Renewable Energy Systems for Oakland University. *Energies*, *16*(15). https://doi.org/https://doi.org/10.3390/en16155830

Alqahtani, B. J., & Patino-Echeverri, D. (2023). Identifying economic and clean strategies to provide electricity in remote rural areas: Main-grid extension vs. Distributed electricity generation. *Energies*, *16*(2), 958. https://doi.org/https://doi.org/10.3390/en16020958

Ampah, J. D., Jin, C., Agyekum, E. B., Afrane, S., Geng, Z., Adun, H., Yusuf, A. A., Liu, H., & Bamisile, O. (2023). Performance analysis and socio-enviro-economic feasibility study of a new hybrid energy system-based decarbonization approach for coal mine sites. *Science of the Total Environment*, *854*(June 2022), 158820. https://doi.org/10.1016/j.scitotenv.2022.158820

Aryani, D. R., Song, H., & Cho, Y.-S. (2022). Operation strategy of battery energy storage systems for stability improvement of the Korean power system. *Journal of Energy Storage*, *56*, 106091. https://doi.org/https://doi.org/10.1016/j.est.2022.106091

Atkinson, J., & Albayati, I. M. (2021). Impact of the generation system parameters on the frequency response of the power system: A UK grid case study. *Electricity*, *2*(2), 143–157. https://doi.org/https://doi.org/10.3390/electricity2020009

Azhar, I. F., Putranto, L. M., & Hadi, S. P. (2020). Design of Battery Energy Storage System Control Scheme for Frequency Regulation for PV Integrated Power System. *Proceeding - 1st FORTEI-International Conference on Electrical Engineering, FORTEI-ICEE 2020*, 7–12. https://doi.org/10.1109/FORTEI-ICEE50915.2020.9249865

Badan Pusatat Statistik Kabupaten Raja Ampat. (2020). *Kabupaten Raja Ampat dalam Angka*. https://rajaampatkab.bps.go.id/publication/2020/04/27/a323a8fc32d8d448c6adc860/kabupaten-raja-ampat-dalam-angka-2020.html

Bank Indonesia. (2023). *Inflation Data*. https://www.bi.go.id/en/statistik/indikator/data-inflasi.aspx

Barco-Jiménez, J., Córdoba, A., Escobar Rosero, E., Pantoja, A., & Caicedo Bravo, E. F. (2022). Optimal sizing of a grid-connected microgrid and operation validation using HOMER Pro and DIgSILENT. *Scientia et Technica*, *27*(1), 28–34. https://doi.org/10.22517/23447214.24965

Bryant, J. S., Sokolowski, P., Jennings, R., & Meegahapola, L. (2021). Synchronous Generator Governor Response: Performance Implications under High Share of Inverter-Based Renewable Energy Sources. *IEEE Transactions on Power Systems*, *36*(3), 2721–2724. https://doi.org/10.1109/TPWRS.2021.3054251

Cárdenas Guerra, C. A., Ospino Castro, A. J., & Peña Gallardo, R. (2023). Analysis of the Impact of Integrating Variable Renewable Energy into the Power System in the Colombian Caribbean Region. *Energies*, *16*(21). https://doi.org/10.3390/en16217260

Chamorro, H. R., Orjuela-Cañón, A. D., Ganger, D., Persson, M., Gonzalez-Longatt, F., Sood, V. K., & Martinez, W. (2020). Nadir frequency estimation in low-inertia power systems. *2020 IEEE 29th International Symposium on Industrial Electronics (ISIE)*, 918–922. https://doi.org/https://doi.org/10.1109/ISIE45063.2020.9152296

Chavez, H., Baldick, R., & Sharma, S. (2014). Governor rate-constrained OPF for primary frequency control adequacy. *IEEE Transactions on Power Systems*, *29*(3), 1473–1480. https://doi.org/10.1109/TPWRS.2014.2298838

Denholm, P., Mai, T., Kenyon, R. W., Kroposki, B., & Malley, M. O. (2020). Inertia and the Power Grid : A Guide Without the Spin. *National Renewable Energy Laboratory*, *May*, 48. https://www.nrel.gov/docs/fy20osti/73856.pdf

Elhassan, Z. A. (2023). Utilizing Homer Power Optimization Software for A Techno-Economic Feasibility, Study of a Sustainable Grid-Connected Design for Urban Electricity in, Khartoum. *Metallurgical and Materials Engineering*, *29*(1), 101–118. https://doi.org/10.56801/MME988

Gholami, M., Sanjari, M. J., Safari, M., Akbari, M., & Kamali, M. R. (2020). Static security assessment of power systems: A review. *International Transactions on Electrical Energy Systems*, *30*(9), 1–23. https://doi.org/10.1002/2050-7038.12432

Hawas, M. N., Hasan, I. J., & Mnati, M. J. (2022). Simulation and analysis of the distributed photovoltaic generation systems based on DIgSILENT power factory. *Indonesian Journal of Electrical Engineering and Computer Science*, *28*(3), 1227–1238. https://doi.org/10.11591/ijeecs.v28.i3.pp1227-1238

HOMER Energy. (2017). *HOMER Pro 3.10*. https://www.homerenergy.com/products/pro/docs/3.10/index.html

Ishraque, M. F., Rahman, A., Shezan, S. A., & Shafiullah, G. (2022). Operation and Assessment of a Microgrid for Maldives: Islanded and Grid-Tied Mode. *Sustainability*, *14*(23), 15504. https://doi.org/10.3390/su142315504

Kanata, S., Baqaruzi, S., Muhtar, A., Prasetyawan, P., & Winata, T. (2021). Optimal planning of hybrid renewable energy system using Homer in Sebesi Island, Indonesia. *International Journal of Renewable Energy Research (IJRER)*, *11*(4), 1507–1516. https://doi.org/https://doi.org/10.20508/ijrer.v11i4.12296.g8303

Kundur, P. (2007). *Power System Stability* (Vol. 10). CRC Press New York.

Kwon, H. Il, Cho, Y. S., & Choi, S. M. (2020). A study on optimal power system reinforcement measures following renewable energy expansion. *Energies*, *13*(22), 1–35. https://doi.org/10.3390/en13225929

Lasseter, R. H., Chen, Z., & Pattabiraman, D. (2020). Grid-Forming Inverters: A Critical Asset for the Power Grid. *IEEE Journal of Emerging and Selected Topics in Power Electronics*, *8*(2), 925–935. https://doi.org/10.1109/JESTPE.2019.2959271

López-Castrillón, W., Sepúlveda, H. H., & Mattar, C. (2021). Off-grid hybrid electrical generation systems in remote communities: Trends and characteristics in sustainability solutions. *Sustainability*, *13*(11), 5856. https://doi.org/https://doi.org/10.3390/su13115856

Matsumoto, K., & Matsumura, Y. (2022). Challenges and economic effects of introducing renewable energy in a remote island: A case study of Tsushima Island, Japan. *Renewable and Sustainable Energy Reviews*, *162*, 112456. https://doi.org/10.1016/j.rser.2022.112456

Mehta, S., & Basak, P. (2020). A Case Study on PV Assisted Microgrid Using HOMER Pro for Variation of Solar Irradiance Affecting Cost of Energy. *2020 IEEE 9th Power India International Conference (PIICON)*, 1–6. https://doi.org/10.1109/PIICON49524.2020.9112894

Ministry of Energy and Mineral Resources; Danish Energy Agency. (2021). *Technology Data for the Indonesian Power Sector*. *February*, 1–215. https://ens.dk/sites/ens.dk/files/Globalcooperation/technology_data_for_the_indonesian_power_sector_-_final.pdf

National Aeronautics and Space Administration (NASA) Langley Research Center (LRac). (2022). *Prediction of Worldwide Energy Resource (POWER) Project*.

PT PLN (Persero). (2020). *Konversi PLTD 225 MW di 200 Lokasi Berbasis Energi Baru & Terbarukan (Conversion of 225 MW Diesel Power Plants at 200 Locations Based on New & Renewable Energy)*.

PT PLN (Persero). (2023). Statistik PLN 2022. In *Statistik PLN* (Issue 03001).

Putranto, L. M., Putra, E. N., Budi, R. F. S., & Nugraha, C. F. (2021). Generation and Transmission Expansion Planning in Remote Areas by considering Renewable Energy Policy and Local Energy Resources: The Case Study of Jayapura Power System. *2021 3rd International Conference on High Voltage Engineering and Power Systems (ICHVEPS)*, 143–148. https://doi.org/https://doi.org/10.1109/ICHVEPS53178.2021.9600932

Rathnayake, D. B., Akrami, M., Phurailatpam, C., Me, S. P., Hadavi, S., Jayasinghe, G., Zabihi, S., & Bahrani, B. (2021). Grid forming inverter modeling, control, and applications. *IEEE Access*, *9*, 114781–114807. https://doi.org/https://doi.org/10.1109/ACCESS.2021.3104617

Renugen. (2024). *Ryse Energy E-10 10kW Wind Turbine*. https://store-7wpeis.mybigcommerce.com/ryse-energy-e-10-10kw-wind-turbine/

Riayatsyah, T. M. I., Geumpana, T. A., Fattah, I. M. R., & Mahlia, T. M. I. (2022). Techno-Economic Analysis of Hybrid Diesel Generators and Renewable Energy for a Remote Island in the Indian Ocean Using HOMER Pro. *Sustainability (Switzerland)*, *14*(16). https://doi.org/10.3390/su14169846

Roy, D. (2023). Modelling an off-grid hybrid renewable energy system to deliver electricity to a remote Indian island. *Energy Conversion and Management*, *281*(January), 116839. https://doi.org/10.1016/j.enconman.2023.116839

Russian Federation. (2014). *State Standard GOST 32144-2013*.

Ryse Energy. (2020). *E-10 Data Sheet*.

See, A. M. K., Mehranzamir, K., Rezania, S., Rahimi, N., Afrouzi, H. N., & Hassan, A. (2022). Techno-economic analysis of an off-grid hybrid system for a remote island in Malaysia: Malawali island, Sabah. *Renewable and Sustainable Energy Transition*, *2*, 100040. https://doi.org/https://doi.org/10.1016/j.rset.2022.100040

Setyowati, A. B. (2020). Mitigating energy poverty: Mobilizing climate finance to manage the energy trilemma in Indonesia. *Sustainability*, *12*(4), 1603. https://doi.org/https://doi.org/10.3390/su12041603

Shezan, S. A., Ishraque, M. F., Muyeen, S. M., Arifuzzaman, S. M., Paul, L. C., Das, S. K., & Sarker, S. K. (2022). Effective dispatch strategies assortment according to the effect of the operation for an islanded hybrid microgrid. *Energy Conversion and Management: X*, *14*(January), 100192. https://doi.org/10.1016/j.ecmx.2022.100192

Simic, N., Strezoski, L., & Dumnic, B. (2021). Short-circuit analysis of DER-based microgrids in connected and islanded modes of operation. *Energies*, *14*(19), 6372. https://doi.org/https://doi.org/10.3390/en14196372

Subekti, L., Nugraha, C. F., Arrofiq, M., Muthahhari, A. A., Prasetyo, B. E., & Qurrota, A. (2024). A Techno-Economic Analysis for Raja Ampat Off-Grid System. *Jurnal Nasional Teknik Elektro*, *1*. https://doi.org/https://doi.org/10.25077/jnte.v13n1.1180.2024

Syafrianto, D., Banjar-Nahor, K. M., Nugraha, H., Hakam, D. F., Hadi, P. O., & Hariyanto, N. (2021). Optimized Hybrid Power System Configuration for the First Phase of Dedieselization Programs. *2021 3rd International Conference on High Voltage Engineering and Power Systems, ICHVEPS 2021*, 387–392. https://doi.org/10.1109/ICHVEPS53178.2021.9601010

Trina Solar Limited. (2020). *TSM-DE08M.08(II)*. https://static.trinasolar.com/sites/default/files/EU_Datasheet_HoneyM_DE08M.08%28II%29_2021_A.pdf

World Bank. (2022). *Population, total - Indonesia*. https://data.worldbank.org/indicator/SP.POP.TOTL?locations=ID

Xu, A., Awalin, L. J., Al-Khaykan, A., Fard, H. F., Alhamrouni, I., & Salem, M. (2023). Techno-Economic and Environmental Study of Optimum Hybrid Renewable Systems, including PV/Wind/Gen/Battery, with Various Components to Find the Best Renewable Combination for Ponorogo Regency, East Java, Indonesia. *Sustainability (Switzerland)*, *15*(3). https://doi.org/10.3390/su15031802

Xu, G., Chen, Z., Zhu, H., Wang, C., Hou, W., & Zhu, X. (2021). Fast frequency regulation strategy for improving frequency stability of off-grid microgrid. *China International Conference on Electricity Distribution, CICED*, *2021-April*(202005300000008), 568–574. https://doi.org/10.1109/CICED50259.2021.9556739

Zebra, E. I. C., van der Windt, H. J., Nhumaio, G., & Faaij, A. P. C. (2021). A review of hybrid renewable energy systems in mini-grids for off-grid electrification in developing countries. *Renewable and Sustainable Energy Reviews*, *144*, 111036. https://doi.org/https://doi.org/10.1016/j.rser.2021.111036